
Pathway for the Production of Neutron-Rich Isotopes around the $N = 126$ Shell Closure

Y. X. Watanabe,^{1,*} Y. H. Kim,^{2,3,†} S. C. Jeong,^{1,‡} Y. Hirayama,¹ N. Imai,^{1,§} H. Ishiyama,^{1,‡} H. S. Jung,¹ H. Miyatake,¹ S. Choi,^{2,3} J. S. Song,^{2,3,4} E. Clement,⁵ G. de France,⁵ A. Navin,^{5,||} M. Rejmund,⁵ C. Schmitt,⁵ G. Pollarolo,⁶ L. Corradi,⁷ E. Fioretto,⁷ D. Montanari,⁸ M. Niikura,^{9,¶} D. Suzuki,^{9,**} H. Nishibata,¹⁰ and J. Takatsu¹⁰

¹*Institute of Particle and Nuclear Studies, High Energy Accelerator Research Organization (KEK), Tsukuba, Ibaraki 305-0801, Japan*

²*Department of Physics and Astronomy, Seoul National University, Seoul 08826, Korea*

³*Institute for Nuclear and Particle Astrophysics, Seoul National University, Seoul 08826, Korea*

⁴*Institute for Basic Science, Daejeon 34047, Korea*

⁵*Grand Accélérateur National d'Ions Lourds (GANIL), F-14076 Caen Cedex 5, France*

⁶*Dipartimento di Fisica Teorica, Università di Torino, and Istituto Nazionale di Fisica Nucleare, I-10125 Torino, Italy*

⁷*Istituto Nazionale di Fisica Nucleare, Laboratori Nazionali di Legnaro, I-35020 Legnaro, Italy*

⁸*Dipartimento di Fisica, Università di Padova, and Istituto Nazionale di Fisica Nucleare, I-35131 Padova, Italy*

⁹*Institut de Physique Nucléaire (IPN), IN2P3-CNRS, F-91406 Orsay Cedex, France*

¹⁰*Department of Physics, Osaka University, Osaka 560-0043, Japan*

(Received 26 June 2015; published 23 October 2015)

Absolute cross sections for isotopically identified products formed in multinucleon transfer in the $^{136}\text{Xe} + ^{198}\text{Pt}$ system at ~ 8 MeV/nucleon are reported. The isotopic distributions obtained using a large acceptance spectrometer demonstrated the production of the “hard-to-reach” neutron-rich isotopes for $Z < 78$ around the $N = 126$ shell closure far from stability. The main contribution to the formation of these exotic nuclei is shown to arise in collisions with a small kinetic energy dissipation. The present experimental finding corroborates for the first time recent predictions that multinucleon transfer reactions would be the optimum method to populate and characterize neutron-rich isotopes around $N = 126$ which are crucial for understanding both astrophysically relevant processes and the evolution of “magic” numbers far from stability.

Nuclei far from the valley of stability provide new vistas for searching and understanding the simple and regular patterns that are found in the structure of complex nuclei. The extremes of the nuclear landscape not only allow us to examine specific aspects of the nuclear interaction but also provide important inputs for the understanding of astrophysically important processes. Approximately half of the nuclei in nature heavier than iron are considered to be synthesized by the rapid neutron capture process (r process), which proceeds under the stellar environment of high neutron densities and high temperatures [1]. The remnants on the r -process path decay to the valley of the β stability and the observed solar r -abundance distribution shows a peak around the mass number (A) 195, which is considered to originate from the waiting point nuclei with the “magic” neutron number $N = 126$. The properties of these nuclei, unknown so far, are necessary to explore the evolution of magic numbers far from the valley of β stability [2]. The experimental information on the neutron-rich nuclei around $N = 126$ is extremely scarce for $Z \leq 80$ due to limited methods for their production.

Conventionally, fusion, fission, and fragmentation are used for the production of neutron-rich isotopes [3]. For the specific case of the production of neutron-rich nuclei near $N = 126$ and beyond, (i) the lack of relevant stable beams and targets precludes using fusion for the production of

isotopes with $Z < 82$, (ii) the production cross section would be extremely small through very asymmetric fission, and (iii) the fragmentation of Pb suffers from rapidly decreasing cross sections for $N = 126$ for $Z < 82$. The fragmentation of a heavier projectile like U also results in a strong decrease in cross sections with proton removal. An alternative path of producing neutron-rich nuclei far from stability via multiple transfer processes using next generation radioactive beam facilities was discussed in Ref. [4]. More recently, it has been predicted that using stable beams, the same mechanism can be employed to populate this unexplored area around $N = 126$ [5]. The proposed method takes advantage of the exchange of a large number of nucleons between two heavy ions at energies around the Coulomb barrier in collisions ranging from peripheral [6] to close collisions [7]. A lot of expectation for achieving the goal rides on the reliability of these predictions, which have not been verified yet or even truly addressed due to challenges in the associated measurements involving a direct isotopic identification at low energies of these heavy reaction products over a wide energy and angular range.

Because of the expected stabilizing effect of closed neutron shells in both nuclei, the collisions of ^{136}Xe with ^{208}Pb have been proposed [5]. The use of ^{136}Xe beams is advantageous over lighter projectiles as its N/Z ratio ($N/Z = 1.52$) is large and similar to that of the target

nucleus ^{208}Pb ($N/Z = 1.54$). The production of neutron-rich nuclei via the $^{136}\text{Xe} + ^{208}\text{Pb}$ system was studied at Dubna at energies around the Coulomb barrier [8]. The measured mass distributions of the targetlike fragments (TLFs) showed a long tail that extended up to almost 240 mass units for low total kinetic energy losses (TKELs), indicating a large nucleon transfer and high survival probability of these products. The unmeasured atomic charge and the poor mass resolution (7 mass units) precluded isotopic identification except for three isotopes with $Z > 82$, which were identified by α decay. At GSI, the $^{64}\text{Ni} + ^{207}\text{Pb}$ system at 5 MeV/nucleon was used to populate nuclei around Pb [9]. Several transfer products on the neutron-rich side were identified; however, new isotopes were not observed. Indirect measurements of cross sections for neutron-rich nuclei, using characteristic γ rays detected with the Gammasphere, in the $^{136}\text{Xe} + ^{208}\text{Pb}$ system have just been reported [10]. As this method requires the knowledge of the level schemes, it precludes the search for new isotopes. Based on the pattern of the identified production, the authors of Ref. [10] suggest a further test of the predictions of Ref. [5].

The advent of large acceptance magnetic spectrometers for heavy ion reactions such as VAMOS++ [11] and PRISMA [12] has now made it possible for a direct and unique isotopic identification of heavy fragments at energies around the Coulomb barrier [13,14]. Calculations using the GRAZING code [15] predict larger cross sections for neutron-rich isotopes with a ^{136}Xe beam on a ^{198}Pt ($N/Z = 1.54$) target as compared to ^{208}Pb because of the larger transfer probabilities of neutrons compared to protons. A recent modification of GRAZING by Yanez and Loveland [16], GRAZING-F, which takes into account fission decay of the primary fragments, also demonstrated a further advantage of the ^{198}Pt target, namely, a negligible effect of fission.

We report here the first successful measurements for the production of neutron-rich isotopes of $N = 126$ and higher in multinucleon transfer (MNT) between two heavy ions. Using the advantages of a large acceptance high resolution mass spectrometer, the first direct measurements of the absolute production cross sections for a large number of fragments in the reaction $^{136}\text{Xe} + ^{198}\text{Pt}$ at the energy above the Coulomb barrier were achieved. The work represents a substantial advance to address the potential of the new isotope production by MNT reactions at both present and future facilities [17].

The measurements were carried out at GANIL in Caen. A beam of $^{136}\text{Xe}^{20+}$ ions was directed at a foil of 1.3 mg/cm^2 ^{198}Pt (91.6% enriched) with an energy of 7.98 MeV/nucleon ($\sim 55\%$ higher than the Coulomb barrier) and a typical intensity of 0.25 pA. The projectile-like fragments (PLFs) around the grazing angle ($\sim 33^\circ$) were detected by the spectrometer VAMOS++ placed at 30° with respect to the beam axis with an angular opening of

$\pm 7^\circ$. VAMOS++ [11,18] consists of a pair of quadrupole magnets, a dipole magnet, and a detection system to determine the scattering angle, kinetic energy, ionic charge, mass, and atomic number of the detected particle. The EXOGAM array [19] with ten CLOVER germanium detectors, surrounding the target, was used to detect γ rays from the PLFs and TLFs. The experimental setup and preliminary results of this measurement can be found in conference proceedings [20,21].

Obtaining absolute cross sections for isotopically identified fragments from a large acceptance spectrometer is demanding and there have not been too many such studies reported. In the present work, the acceptance of the spectrometer for detected particles with different magnetic rigidities and scattering angles was evaluated using the ion optical code ZGOUBI [22]. Absolute normalization was obtained by comparing the elastic scattering to the Rutherford cross section at forward angles (24° – 27°), where the transfer and deep inelastic collision (DIC) components are negligible. The energy distribution of the ^{136}Xe ions at each angle was fitted to three Gaussian distributions corresponding to the elastic, quasielastic, and DIC. The elastic events accounted for more than 99% of the total events. These cross sections as a function of the scattering angle are shown in Fig. 1(a). The solid line shows the corresponding optical model fit using the code PTOLEMY [23] with a derived total reaction cross section of 2899 mb. The best fit parameters for the nuclear potential were $V_0 = -30 \text{ MeV}$, $a = 0.6 \text{ fm}$, and $r_0 = 1.21 \text{ fm}$ (real part), $V_{10} = -20 \text{ MeV}$, $a_1 = 0.4 \text{ fm}$, and $r_{10} = 1.30 \text{ fm}$ (imaginary part). The absolute cross sections for the detected PLFs are shown by filled circles in Figs. 1(b)–(j). These were obtained by integrating the measured angular distributions from 24° to 34° . The derived reaction cross section was found to be in good agreement with the summation of the measured cross sections $(2.7 \pm 1.0) \times 10^3 \text{ mb}$ for PLFs shown in Fig. 1 (excluding elastic scattering), confirming the normalization procedure. The error bars shown are typically $\sim 25\%$ and include acceptance correction ($\sim 15\%$), extrapolation of the ionic charge distribution ($\sim 5\%$), particle identification ($\sim 0.3\%$), statistics ($\sim 3\%$), and normalization ($\sim 20\%$).

Figure 1 shows that the proton pick-up channels have larger cross sections at their maxima than those for the corresponding proton stripping channels. As more protons are stripped, the mass number at the peak drifts to lower A as compared to the pure proton transfer channels (with no neutrons transfer, indicated by arrows). This shift of the peak is 12 neutrons lower as compared to pure proton stripping in the $-4p$ transfer case. On the other hand, for the proton pick-up channels, the shift of the distribution was found to be only one neutron compared to the corresponding pure proton pickup. It should be pointed out that the shift of A from pure proton transfer channels is not a direct indication of the number of transferred neutrons. This is because the measured PLFs are remnants,

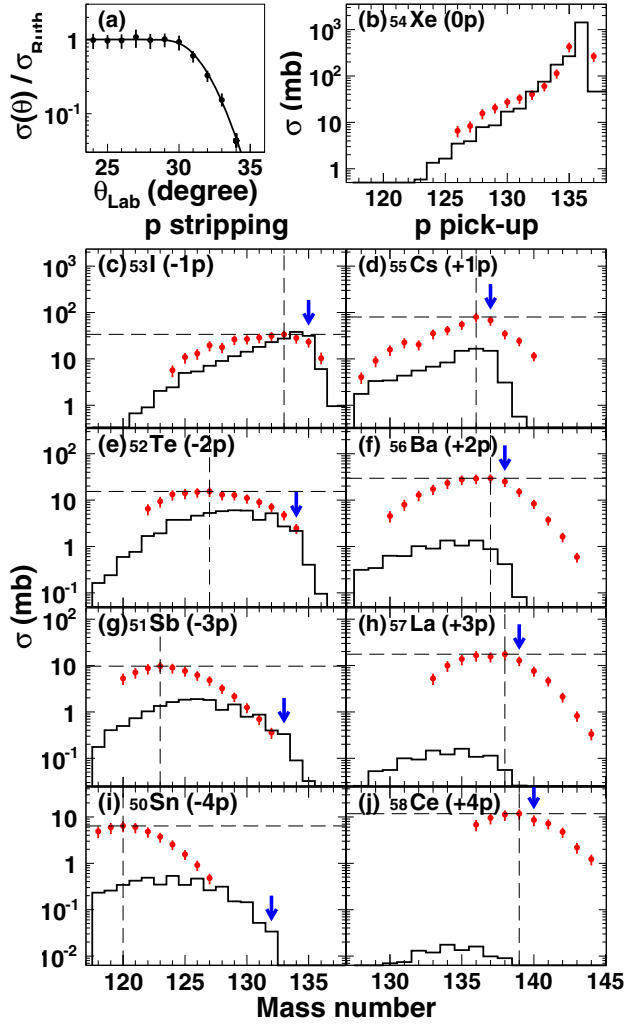


FIG. 1 (color online). (a) Ratio of differential cross section for elastic to Rutherford scattering as a function of the angle in the laboratory system. The curve represents optical model calculations (see text). (b)–(j) Angle and Q -value integrated cross sections for the various projectilelike fragments measured in the present work. The histograms represent the corresponding calculations. The cross sections and masses at the maximum of the isotopic distributions for proton transfer channels are indicated by horizontal and vertical dashed lines, respectively. The position of pure proton transfer is indicated by the arrows.

after neutron evaporation, of the excited primary PLFs. However, the large (small) shifts of the peak positions from the corresponding pure proton transfer channels with increasing number of stripped (picked-up) protons suggest that neutron transfer accompanies proton transfer. This tendency becomes more striking when the data are compared with GRAZING calculations shown by histograms in Figs. 1(b)–1(j). GRAZING calculates the evolution of the reaction by taking into account, besides the relative motion, the intrinsic degrees of freedom of projectile and target. These are the isoscalar surface modes and the single-nucleon transfer channels. The multinucleon transfer

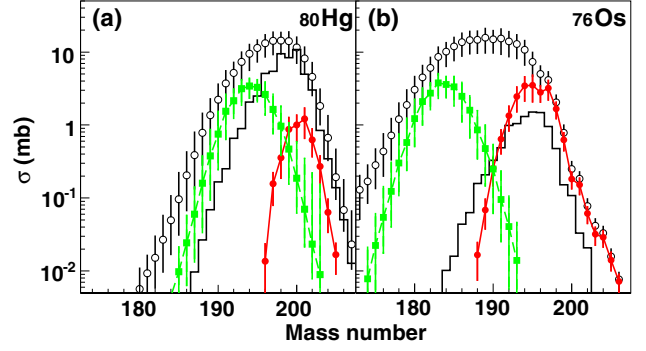


FIG. 2 (color online). Experimentally deduced (open circles) and calculated by GRAZING (histograms) cross sections for Hg (left) and Os (right) isotopes. Isotopic distributions for different windows of total kinetic energy loss from -25 to 25 MeV and from 175 to 225 MeV are indicated by different filled symbols of circles and squares, respectively.

channels are described via a multistep mechanism. The relative motion of the system is calculated in a nuclear plus Coulomb field, where for the nuclear part the empirical potential of Ref. [24] has been used. The excitation of the intrinsic degrees of freedom is obtained by employing standard form factors for the collective surface vibrations and the one-particle transfer channels [6,25]. The model, to calculate the isotopic distributions of the produced fragments, takes into account, in a simple way, the effect of neutron evaporation. The measured distributions peak at lower and higher A values for proton stripping and pick-up channels, respectively, as compared to the calculations. It should be emphasized that the code calculates only the direct component of the MNT by taking into account only a small range of impact parameters close to the grazing where most of the cross section is concentrated in the quasielastic scattering. The contributions coming from small impact parameters, leading to DIC, are not considered. The difference from the calculation indicates that the fragment isotopic distributions have large contributions associated with strong energy damping in the DIC at this energy above the Coulomb barrier. As the charge equilibration is unfavorable for production of neutron-rich TLFs, one has to instead rely on “direct” reactions at reasonably small excitation energies (so as to minimize the particle evaporation).

The production of the neutron-rich TLFs around the $N = 126$ shell closure was deduced from the measured energies and angles of the PLFs in the following iterative manner. Initially, the detected PLF is assumed to be the primary PLF (before evaporation) in the ground state and thus the primary TLF and its excitation energy were deduced using binary kinematics with conservation of the total Z , A , energy, and momentum (using the measured velocity vector). The TKEL is obtained by subtracting the ground state Q value from the total of the above deduced excitation energy of the TLF and the assumed excitation energy of the PLF

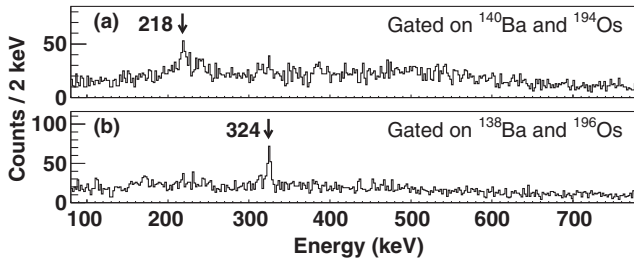


FIG. 3. Doppler corrected γ -ray spectra for $^{194,196}\text{Os}$ gated on $^{140,138}\text{Ba}$ for PLFs and the deduced $^{194,196}\text{Os}$ for TLFs, respectively.

(which was 0 in the first iteration). This new total excitation energy is further shared between the two deduced primary fragments, in proportion to their masses. The number of evaporated neutrons from the primary PLFs is then calculated from its excitation energy using PACE4 [26], and its A is deduced by adding the evaporated neutron number to the A of the detected PLF. Using this primary PLF mass at a finite excitation energy, the binary kinematics condition is again used to deduce the primary TLF in an iterative manner. These iterations are repeated until the deduced excitation energy of the PLF converged, and then the TLF was deduced by subtracting evaporated particles from the primary TLF using PACE4. The standard deviations of the calculated distributions for the number of evaporated neutrons were included in the estimation of the uncertainties in the cross sections of the TLFs.

Figure 2 shows the so experimentally deduced TLF cross sections for the $-2p$ and $+2p$ channels corresponding to the Hg and Os isotopes, respectively. Also shown are the isotopic distributions for two different TKEL partitions. There is a good agreement between the data and the calculations for the relatively more neutron-rich nuclei (large A). As can be seen, the production of the very neutron-rich nuclei produced in the pick-up channel (Os) dominantly arises from low TKEL. Higher TKEL contributes to the production of neutron-deficient isotopes. Such components are not included in the GRAZING calculations, showing the large discrepancies at the neutron-deficient side and the modest ones at the neutron-rich side. The proton pick-up channels show relatively large discrepancy from the calculations on the neutron-rich side. This was also observed in other cases [27] and cannot be explained by the DIC component, indicating that GRAZING is underestimating the magnitude of the matrix elements (form factors) for the proton pick-up channel. The predominant contribution of the lowest TKEL components for production of the neutron-rich nuclei around $N = 126$ by the proton pickup implies that a small number of neutrons (< 2) are evaporated. This indicates a small uncertainty arising from the procedure and parameters used in the PACE4 calculations in the determination of the A of the TLFs and their corresponding cross sections. The procedure for obtaining the TLF was further validated from the measurement of the characteristic γ rays for the more

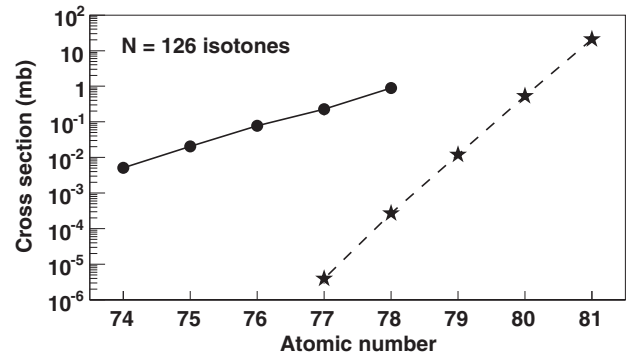


FIG. 4. Experimentally deduced cross sections for the production of the $N = 126$ isotones as a function of the atomic number. The filled circles are from the present work and the filled stars are from the fragmentation of $^{208}\text{Pb}(1 \text{ GeV/nucleon}) + \text{Be}$ [28]. The solid and dashed lines are to guide the eye.

difficult cases where higher TKEL components contribute. Figure 3 shows the Doppler corrected γ -ray spectra for $^{194,196}\text{Os}$ isotopes gated on the relevant Ba as PLFs and the deduced Os as TLFs.

Figure 4 shows the comparison of the experimentally deduced cross sections using the present work based on MNT and those recently measured in the fragmentation of a 1 GeV/nucleon ^{208}Pb beam on a Be target [28]. The huge advantage of the current approach using MNT for the production of very neutron-rich nuclei with $Z \leq 77$ can be clearly seen. It demonstrates that the MNT route is a more promising path to produce and characterize $N = 126$ neutron-rich isotopes. The relative comparison of the production rate with a 2 mg/cm² ^{198}Pt target and 20 pA Xe beam as compared to that from fragmentation of $^{208}\text{Pb}(1 \text{ GeV/nucleon}, 1 \text{ pA}) + \text{Be}(5 \text{ g/cm}^2)$ also shows that the former would be a more optimum way of production of these interesting nuclei. Further assuming a $\sim 5\%$ extraction efficiency by using a gas catcher system with laser resonance ionization technique, the method of MNT to produce ISOL beams would make lifetime measurements of these nuclei feasible [17].

In conclusion, the promised potential of the production of new isotopes around and beyond the neutron shell $N = 126$ by multinucleon transfer reactions was established for the first time in the $^{136}\text{Xe} + ^{198}\text{Pt}$ system at an energy above the Coulomb barrier. The absolute cross sections of targetlike fragments over a range of isotopes extending up to $N \geq 126$ were deduced from the measured isotopically identified projectilelike fragments. The most neutron-rich nuclei were observed to be produced mainly through collisions involving a small kinetic energy loss. The expected production rates of the neutron-rich isotopes at $N = 126$ with $Z \leq 77$ from the measured cross sections demonstrate the possibility of producing them as ISOL beams. The advantage becomes more and more striking when the atomic number is lower, approaching the r -process nuclei. The use of low energy beams along with

the large cross sections for their production opens the possibility of characterizing the properties of these unknown nuclei, including those of the excited states (using next generation gamma-tracking detectors) to understand the evolution of nuclear structure far from stability.

The authors gratefully acknowledge the important technical contributions of J. Goupil, G. Fremont, L. Ménager, J. Ropert, C. Spitaels, and the GANIL accelerator staff, and B. Jacquot for a critical reading of the manuscript. This work was supported by JSPS KAKENHI Grant No. 23244060.

*yutaka.watanabe@kek.jp

†Present address: Grand Accélérateur National d'Ions Lourds (GANIL), F-14076 Caen Cedex 5, France.

*Present address: Institute for Basic Science, Daejeon 34047, Korea.

§Present address: Center for Nuclear Study, University of Tokyo, Tokyo 113-0033, Japan.

||navin@ganil.fr

†Present address: Department of Physics, University of Tokyo, Tokyo 113-0033, Japan.

**Present address: RIKEN Nishina Center, Wako, Saitama 351-0198, Japan.

- [1] H. Grawe, L. Langanke, and G. Martínez-Pinedo, Nuclear structure and astrophysics, *Rep. Prog. Phys.* **70**, 1525 (2007).
- [2] O. Sorlin and M.-G. Porquet, Nuclear magic numbers: New features far from stability, *Prog. Part. Nucl. Phys.* **61**, 602 (2008).
- [3] M. Thoennessen, Discovery of Nuclides Project, <https://people.nscf.msu.edu/~thoennessen/isotopes/>.
- [4] C. H. Dasso, G. Pollarolo, and A. Winther, Systematics of Isotope Production with Radioactive Beams, *Phys. Rev. Lett.* **73**, 1907 (1994); Particle evaporation following multinucleon transfer processes with radioactive beams, *Phys. Rev. C* **52**, 2264 (1995).
- [5] V. Zagrebaev and W. Greiner, Production of New Heavy Isotopes in Low-Energy Multinucleon Transfer Reactions, *Phys. Rev. Lett.* **101**, 122701 (2008).
- [6] R. A. Broglia, G. Pollarolo, and A. Winther, On the absorptive potential in heavy ion scattering, *Nucl. Phys.* **A361**, 307 (1981).
- [7] V. V. Volkov, Deep inelastic transfer reactions – The new type of reactions between complex nuclei, *Phys. Rep.* **44**, 93 (1978).
- [8] E. M. Kozulin *et al.*, Mass distributions of the system $^{136}\text{Xe} + ^{208}\text{Pb}$ at laboratory energies around the Coulomb barrier: A candidate reaction for the production of neutron-rich nuclei at $N = 126$, *Phys. Rev. C* **86**, 044611 (2012).
- [9] O. Beliuskina *et al.*, On the synthesis of neutron-rich isotopes along the $N = 126$ shell in multinucleon transfer reactions, *Eur. Phys. J. A* **50**, 161 (2014).
- [10] J. S. Barrett *et al.*, $^{136}\text{Xe} + ^{208}\text{Pb}$ reaction: A test of models of multinucleon transfer reactions, *Phys. Rev. C* **91**, 064615 (2015).
- [11] M. Rejmund *et al.*, Performance of the improved larger acceptance spectrometer: VAMOS++, *Nucl. Instrum. Methods Phys. Res., Sect. A* **646**, 184 (2011).
- [12] L. Corradi, G. Pollarolo, and S. Szilner, Multinucleon transfer processes in heavy-ion reactions, *J. Phys. G* **36**, 113101 (2009).
- [13] A. Navin *et al.*, Towards the high spin–isospin frontier using isotopically-identified fission fragments, *Phys. Lett. B* **728**, 136 (2014).
- [14] D. Montanari *et al.*, Neutron Pair Transfer in $^{60}\text{Ni} + ^{116}\text{Sn}$ Far below the Coulomb Barrier, *Phys. Rev. Lett.* **113**, 052501 (2014).
- [15] A. Winther, Grazing reactions in collisions between heavy nuclei, *Nucl. Phys.* **A572**, 191 (1994); Dissipation, polarization and fluctuation in grazing heavy-ion collisions and the boundary to the chaotic regime, *Nucl. Phys.* **A594**, 203 (1995); Program GRAZING, <http://www.to.infn.it/~nanni/grazing/> (unpublished).
- [16] R. Yanez and W. Loveland, Predicting the production of neutron-rich heavy nuclei in multinucleon transfer reactions using a semi-classical model including evaporation and fission competition, GRAZING-F, *Phys. Rev. C* **91**, 044608 (2015).
- [17] S. C. Jeong *et al.*, KISS: KEK isotope separation system for β -decay spectroscopy, KEK Report 2010-2 (High Energy Accelerator Research Organization, 2010).
- [18] S. Pullanhiotan, M. Rejmund, A. Navin, W. Mittig, and S. Bhattacharyya, Performance of VAMOS for reactions near the Coulomb barrier, *Nucl. Instrum. Methods Phys. Res., Sect. A* **593**, 343 (2008).
- [19] J. Simpson *et al.*, The EXOGAM array: A radioactive beam gamma-ray spectrometer, *Acta Phys. Hung. New Ser.: Heavy Ion Phys.* **11**, 159 (2000).
- [20] Y. X. Watanabe *et al.*, Study of collisions of $^{136}\text{Xe} + ^{198}\text{Pt}$ for the KEK isotope separator, *Nucl. Instrum. Methods Phys. Res., Sect. B* **317**, 752 (2013).
- [21] Y. H. Kim *et al.*, Study of the multi-nucleon transfer reactions of $^{136}\text{Xe} + ^{198}\text{Pt}$ for producing exotic heavy nuclei, *Eur. Phys. J. Web Conf.* **66**, 03044 (2014).
- [22] F. Méot, The ray-tracing code Zgoubi, *Nucl. Instrum. Methods Phys. Res., Sect. A* **427**, 353 (1999).
- [23] M. Macfarlane and S. C. Pieper, Argonne National Laboratory Report No. ANL-76-11, 1978.
- [24] R. A. Broglia and A. Winther, *Heavy Ion Reactions*, Frontiers in Physics Lecture Note Series (Addison-Wesley, Redwood City, CA, 1991), Vol. 84.
- [25] G. Pollarolo, R. A. Broglia, and A. Winther, Calculation of the imaginary part of the heavy ion potential, *Nucl. Phys.* **A406**, 369 (1983).
- [26] O. B. Tarasov and D. Bazin, Development of the program LISE: application to fusion–evaporation, *Nucl. Instrum. Methods Phys. Res., Sect. B* **204**, 174 (2003); A. Gavron, Statistical model calculations in heavy ion reactions, *Phys. Rev. C* **21**, 230 (1980).
- [27] L. Corradi, A. M. Stefanini, C. J. Lin, S. Beghini, G. Montagnoli, F. Scarlassara, G. Pollarolo, and A. Winther, Multinucleon transfer processes in $^{64}\text{Ni} + ^{238}\text{U}$, *Phys. Rev. C* **59**, 261 (1999).
- [28] T. Kurtukian-Nieto *et al.*, Production cross sections of heavy neutron-rich nuclei approaching the nucleosynthesis r-process path around $A = 195$, *Phys. Rev. C* **89**, 024616 (2014).